Cent. Eur. J. Phys. • 9(1) • 2011 • 123-130
DOI: 10.2478/s11534-010-0049-1

VERSITA

Central European Journal of **Physics**

Accuracy of Cotton-Mouton polarimetry in sheared toroidal plasma of circular cross-section

Research Article

Yury A. Kravtsov[1,2], Janusz Chrzanowski[2]*

1 *Space Research Institute, Profsoyuznaya St. 82/34, Moscow 117997, Russia*

2 *Institute of Physics, Maritime University of Szczecin, 1-2 Waly Chrobrego St., Szczecin 70500, Poland*

Received 29 January 2010; accepted 26 May 2010

Abstract: The Cotton-Mouton effect in sheared plasma with helical magnetic lines is studied on the basis of the equation for complex amplitude ratio (CAR). A simple model for helical magnetic lines in sheared plasma of toroidal configuration is suggested. The equation for CAR in the sheared plasma is solved by perturbation method, using the small shear angle deviations as is characteristic for tokamak plasma. It is shown that the inaccuracy in polarization measurements caused by deviations of the sheared angle amounts to some percentage of the shearless Cotton-Mouton phase shift. One suggested method is to subtract the "sheared" term, which may improve the accuracy of the Cotton-Mouton measurements in the sheared plasma.

PACS (2008): 52.55.Fa, 52.55.Hc, 52.70.Ds, 52.70.Gw, 52.70.Kz

Keywords: microwave plasma polarimetry • polarization ellipse • complex polarization angle • quasi-isotropic approximation • complex amplitude ratio

1. Introduction

Cotton-Mouton polarimetry deals with transverse propagation of electromagnetic waves with respect to the static magnetic field and measures the phase difference

$$\delta_{CM}(L) = \int_0^L (k_1 - k_2) d\sigma \qquad (1)$$

between two linearly polarized normal modes in magnetoactive plasma [1–4]. Here k_1 and k_2 are propagation constants of the normal modes and σ is an arc length along the sounding ray. The phase difference (1) determines the form of the polarization ellipse, which undergoes analysis in the Cotton-Mouton polarimetry.

Expression (1) for the Cotton-Mouton phase difference is valid under the assumption that magnetic field $\mathbf{B}_0$ preserves its orientation along the sounding ray. However, this is not the case in tokamak plasmas, where magnetic lines formed by the superposition of toroidal and poloidal magnetic fields acquire a helical form [5, 6].

The Cotton-Mouton phenomenon in sheared plasma was studied by Segre [7], who obtained an *exact* solution for

*E-mail: j.chrzanowski@am.szczecin.pl

the Stokes vector in *homogeneous and uniformly sheared plasma*. In contrast to [7], this paper describes an evolution of the electromagnetic wave in *inhomogeneous* and *non-uniformly sheared* plasma. Instead of the Stokes vector formalism (SVF), widely used in plasma polarimetry [7–9], we describe the polarization state of the electromagnetic wave field, using the technique of complex amplitude ratio (CAR). That approach adequately characterizes the parameters of the polarization ellipse [1, 10] similar to other basic polarization characteristics: traditional angular parameters of the polarization ellipse, Stokes vector and complex polarization angle. The equation for CAR evolution in weakly anisotropic plasma was derived in the paper [11] on the basis of the quasi-isotropic approximation (QIA) of geometrical optics [12–16], which provides an asymptotic solution of the Maxwell equations for electromagnetic waves in weakly anisotropic media, including weakly magnetized plasma. The latter manifests properties of a weakly anisotropic medium in millimeter and submillimeter bands of the electromagnetic spectrum, used for polarimetric measurements in modern thermonuclear reactors [5, 6].

This paper is organized as follows. Sect. 2 briefly outlines the QIA approach and involves the equation for CAR. Sect. 3 outlines a simple model for the helical magnetic lines in the sheared plasma of the toroidal configuration [17]. The equation for CAR evolution in the sheared plasma is solved in Sect. 4 by the method of successive approximations. Sect. 4 also analyzes the influence of sheared plasma on the polarization state of the sounding electromagnetic wave and estimates an inaccuracy in polarization measurements, caused by ignoring the magnetic shear in plasma. Sect. 5 suggests a simple method for improving the accuracy in polarimetric measurements, based on a preliminary calculation of the shear angle and its subsequent subtraction from the experimental results.

2. Quasi-isotropic approximation (QIA) and equation for complex amplitudes ratio (CAR) in weakly anisotropic plasma

As mentioned above, the quasi-isotropic approximation (QIA) of geometrical optics method [10–14] provides an asymptotic solution of the Maxwell equations for electromagnetic waves in weakly anisotropic media. The anisotropic part $\nu_{\alpha\beta} = \varepsilon_{\alpha\beta} - \varepsilon_0\delta_{\alpha\beta}$ of the electric permittivity tensor $\varepsilon_{\alpha\beta} = \varepsilon_0\delta_{\alpha\beta} + \nu_{\alpha\beta}$ is considered to be small when compared with the permittivity ε_0 of the background isotropic medium. Weakness in anisotropy is characterized by a small "anisotropic" parameter

$$\mu_A = \frac{\max|\nu_{\alpha\beta}|}{\varepsilon_0} \ll 1,$$

which is used to expand the wave field $\mathbf{E}$ into an asymptotic series along with a traditional small "geometric" parameter

$$\mu_{GO} = \frac{1}{k_0 L} = \frac{\lambda_0}{2\pi L}.$$

Here k_0 and $\lambda_0 = \frac{2\pi}{k_0}$ are refer to a wave number and wavelength in free space, respectively, and L is a characteristic scale of the medium's inhomogeneity.

In the zero-th order of the combined small parameter $\mu = \max(\mu_A, \mu_{GO})$ QIA presents the electromagnetic wave field in the form

$$\mathbf{E} = \mathbf{\Gamma} A(\mathbf{r}) \exp\left[ik_0 \Psi(\mathbf{r})\right], \tag{2}$$

where $\Psi(\mathbf{r})$ and $A(\mathbf{r})$ are the eikonal and amplitude of the scalar wave field in the isotropic medium with background permittivity $\varepsilon_0(\mathbf{r})$.

In the zero-th order of QIA, the polarization vector $\mathbf{\Gamma}$ in Eq. (2) is orthogonal to the ray and can be presented as

$$\mathbf{\Gamma} = \Gamma_1 \mathbf{e}_1 + \Gamma_2 \mathbf{e}_2, \quad \mathbf{e}_1 \perp \mathbf{e}_2 \perp \mathbf{l}, \tag{3}$$

where $\mathbf{l} = \frac{d\mathbf{r}}{d\sigma}$ is a unit vector, tangent to the ray trajectory $\mathbf{r}(\sigma)$, $d\sigma$ is an elementary arc length along the ray and $\mathbf{e}_1$ and $\mathbf{e}_2$ are the unit vectors, orthogonal to the ray trajectory. A convenient choice of the unit vectors $\mathbf{e}_{1,2}$ was suggested by Popov [18]. Let the unit vectors $\mathbf{e}_{1,2}$ take the form

$$\dot{\mathbf{e}}_1 = \mathbf{l}\left(\mathbf{e}_1 \cdot \nabla \ln n\right), \quad \dot{\mathbf{e}}_2 = \mathbf{l}\left(\mathbf{e}_2 \cdot \nabla \ln n\right), \tag{4}$$

where the dot over e indicates a derivative of the arc length σ:

$$\dot{\mathbf{e}}_{1,2} \equiv \frac{d\mathbf{e}_{1,2}}{d\sigma}.$$

According to [18], the unit vectors $\mathbf{e}_{1,2}$ correspond to the orthogonal curvilinear coordinate system, performing a parallel transport of the vector wave field $\mathbf{E}$ along the ray. The parallel transport coordinate system ($\mathbf{e}_1$,$\mathbf{e}_2$, $\mathbf{l}$) is widely used in the theory of open resonators [19], in the theory of transverse elastic waves propagation [20], in complex geometrical optics [21, 22] and within the realms of the QIA approach [23, 24].

The complex amplitudes ratio (CAR) is defined as [1, 10]

$$\zeta = \frac{\Gamma_2}{\Gamma_1}. \tag{5}$$

According to [11], the evolution of CAR in a weakly anisotropic plasma obeys the equation

$$\dot{\zeta} = \frac{1}{2}\left[i\Omega_2\left(1-\zeta^2\right) - 2i\Omega_1\zeta + \Omega_3\left(1+\zeta^2\right)\right]. \quad (6)$$

Here, we use the parameters $\Omega_1, \Omega_2, \Omega_3$, which were involved by Segre (see [7–9]):

$$\begin{cases} \Omega_1 = \frac{k_0 XY^2}{2}\sin^2\alpha_{||}\cos 2\alpha_\perp = \Omega_\perp \cos 2\alpha_\perp = \Omega_{\perp 0}\sin^2\alpha_{||}\cos 2\alpha_\perp, \\ \Omega_2 = \frac{k_0 XY^2}{2}\sin^2\alpha_{||}\sin 2\alpha_\perp = \Omega_\perp \sin 2\alpha_\perp = \Omega_{\perp 0}\sin^2\alpha_{||}\sin 2\alpha_\perp, \\ \Omega_3 = k_0 XY\cos\alpha_{||}. \end{cases} \quad (7)$$

We define the following new parameters

$$\begin{aligned} \Omega_\perp &= \sqrt{\Omega_1^2+\Omega_2^2} = \frac{k_0 XY^2}{2}\sin^2\alpha_{||} = \Omega_{\perp 0}\sin^2\alpha_{||}, \\ \Omega_{\perp 0} &= \frac{k_0 XY^2}{2}, \end{aligned} \quad (8)$$

where $k_0 = \frac{\omega}{c}$ is a wave number in free space. The parameters $\Omega_1, \Omega_2, \Omega_3$ contain the standard plasma parameters X and Y, defined as [2]

$$X = \frac{\omega_p^2}{\omega^2} \equiv \frac{4\pi e^2 N_e}{m\omega^2}, \quad Y = \frac{e\mathbf{B}_0}{mc\omega} = \frac{\omega_c}{\omega} \quad (9)$$

(in the text book [3], they were denoted as v and $\sqrt{u}$, respectively). Here N_e is the electron density, $\mathbf{B}_0$ is the static magnetic field, $\alpha_{||}$ is an angle between the ray and the magnetic vector $\mathbf{B}_0$, and $\alpha_\perp$ is an angle between the unit vector $\mathbf{e}_1$ of the parallel transport coordinate system by Popov [18–24] and the transverse component of the magnetic field $\mathbf{B}_{\perp 0}$, as presented in Fig. 1.

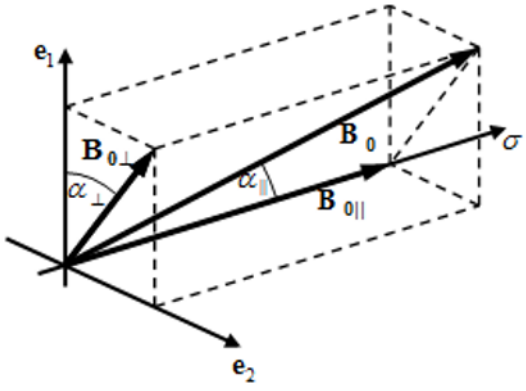

Figure 1. Orientation of the static magnetic field $\mathbf{B}_0$ in the frame of the orthogonal coordinate system, formed by the unit vectors $\mathbf{e}_1$, $\mathbf{e}_2$ and by the axis σ, tangent to the ray.

Following the terminology used in [7], we treat $\alpha_\perp$ as *the shear* angle, because it characterizes the orientation of the transverse component $\mathbf{B}_{\perp 0}$ of the static magnetic field $\mathbf{B}_0$. For electromagnetic waves in the sub-millimeter band, when dealing with plasma polarimetry, the parallel transport coordinate system practically coincides with the Cartesian one. The unit vector $\mathbf{e}_1$ is directed vertically in Fig. 1, and the unit vector $\mathbf{e}_2$ has a horizontal direction. Parameter Ω_3, which linearly depends on magnetic field $\mathbf{B}_0$, describes the Faraday effect. In turn, parameters $\Omega_{1,2}$, $\Omega_\perp$ and $\Omega_{\perp 0}$ are quadratic in $\mathbf{B}_0$ and correspond to the Cotton-Mouton effect [1–4].

3. Simple model for helical magnetic lines in a toroidal system

A convenient model of helical magnetic lines in toroidal plasma was suggested in [17]. Let ϕ be the toroidal angle, calculated from the z axis, θ be the poloidal angle, calculated from the vertical axis x and ρ be the distance from the tor circular axis $R = \text{const}$, where R is a large radius of the toroidal surface (Fig. 2). Cartesian coordinates x, y and z, shown in Fig. 2, can be expressed through the toroidal variables ϕ, ρ and θ as follows:

$$\begin{aligned} x &= \rho\cos\theta, \\ y &= (R+\rho\sin\theta)\sin\phi, \\ z &= (R+\rho\sin\theta)\cos\phi. \end{aligned} \quad (10)$$

Magnetic lines, formed by the toroidal and poloidal magnetic fields, are of helical form, which can be modeled by following the dependence of the poloidal angle θ on the azimuthal angle ϕ:

$$\theta = \theta^0 + \nu\phi = \theta^0 + \nu\frac{\mu}{R}. \quad (11)$$

Here θ^0 is an initial poloidal angle in the x, y plane, corresponding to $\phi = 0$. Instead of toroidal angle ϕ, we

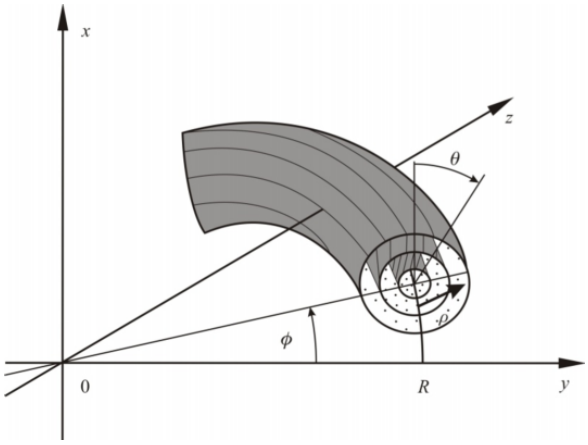

Figure 2. Helical magnetic lines, formed by superposition of the toroidal and poloidal magnetic fields in plasma of toroidal configuration.

shall use a dimensional parameter $\mu = \phi R$, which is an arc length along the circular axis $R = \text{const}$. Finally, parameter ν, which is the rate at which the poloidal angle θ changes along the circular axis, plays a role of the *"helical" factor*. According to Eq. (11), an increment of the poloidal angle θ after one full winding about the vertical axis x is $2\pi\nu$. The helical factor ν happens to be inversely proportional to the *safety factor* q [5, 6]:

$$\nu = \frac{1}{q}. \tag{12}$$

The latter is typically of unit dimension in the vicinity of the circular axis and increases up to 4 on the outer toroidal surface $\rho_{\max} = a$. Correspondingly, the helical factor $\nu = \frac{1}{q}$ takes the values of about one unit in the center of the toroidal system and tends to decrease to $\frac{1}{4}$ at the circular boundary of plasma $\rho_{\max} = a$.

Magnetic lines for the "helical" model (11) can be presented by equations:

$$\begin{cases} x(\mu) = \rho\cos\theta(\mu), \\ y(\mu) = [R + \rho\sin\theta(\mu)]\sin\left(\frac{\mu}{R}\right), \\ z(\mu) = [R + \rho\sin\theta(\mu)]\cos\left(\frac{\mu}{R}\right). \end{cases} \tag{13}$$

According to Eq. (13) vector

$$\mathbf{M} = \left(\frac{dx}{d\mu}, \frac{dy}{d\mu}, \frac{dz}{d\mu}\right),$$

tangent to the magnetic line, is given by

$$\mathbf{M} = \begin{pmatrix} \frac{dx}{d\mu} = -\frac{\rho\nu}{R}\sin\theta, \\ \frac{dy}{d\mu} = \frac{\rho\nu}{R}\cos\theta\sin\frac{\mu}{R} - \left(1 + \frac{\rho}{R}\sin\theta\right)\cos\frac{\mu}{R}, \\ \frac{dz}{d\mu} = \frac{\rho\nu}{R}\cos\theta\cos\frac{\mu}{R} + \left(1 + \frac{\rho}{R}\sin\theta\right)\sin\frac{\mu}{R}. \end{pmatrix}. \tag{14}$$

Let the sounding ray lie in the horizontal plane $x = 0$ and cross the plasma along the y axis, as shown in Fig. 3. Such a ray can be presented by the equations

$$z = -R + \sigma, \quad x = 0, \quad z = 0. \tag{15}$$

Here σ is counted from the point $z = -R$, where the ray crosses the tor circular axis. The point at which the ray enters the plasma will be $\sigma_0 = -a$ and the point of the ray exit will be $\sigma_{\text{exit}} = a$. Correspondingly we have $z_0 = -(R + a)$ and $z_{\text{exit}} = -R + a$.

Note that axis x points in the direction of the unit vector $\mathbf{e}_1$, axis y corresponds to unit vector $\mathbf{e}_2$ and axis z coincides in direction with the unit vector $\mathbf{l}$, tangent to the ray. As a result the complex amplitude ratio

$$\frac{\Gamma_2}{\Gamma_1}$$

takes a traditional form

$$\frac{\Gamma_2}{\Gamma_1} = \frac{\Gamma_y}{\Gamma_x}. \tag{16}$$

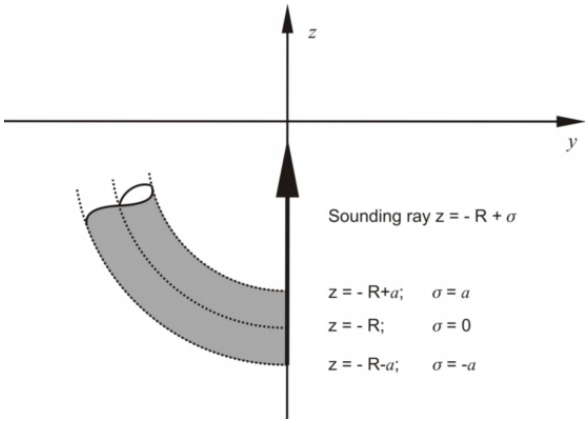

Figure 3. Sounding ray, crossing a toroidal plasma in the (y, z) plane along the z axis.

According to Fig. 1, the cosine of the shear angle $\alpha_\perp$ equals the ratio of the vertical component $\mathbf{B}_{x0}$ of the magnetic field $\mathbf{B}_0$ to the transverse component $\mathbf{B}_{\perp 0}$:

$$\cos\alpha_\perp(\sigma) = \frac{B_{x0}}{B_{\perp 0}} = \frac{M_x}{M_\perp}, \tag{17}$$

where

$$M_x = \frac{\sigma\nu(\sigma)}{R}. \tag{18}$$

According to Eq. (14) the transverse component $M_\perp$ of the vector $\mathbf{M}$ depends on σ in the following way

$$M_\perp = \sqrt{M_x^2 + M_y^2} = \sqrt{\left(\frac{\nu\sigma}{R}\right)^2 + \left(1 - \frac{\sigma}{R}\right)^2}. \tag{19}$$

Here we have taken into account that the combination $\rho\sin\varphi$ is in fact an arc length σ along the ray, counted from the circular axis $z = -R$, and its trajectory (15) corresponds to the poloidal angle $\theta = \frac{\pi}{2}$ at $\sigma < 0$ ($z < -R$) and $\theta = -\frac{\pi}{2}$ at $\sigma > 0$ ($z > -R$). As a result

$$\cos\alpha_\perp(\sigma) = \frac{\sigma\nu(\sigma)}{\sqrt{(\sigma\nu)^2 + (-R+\sigma)^2}}. \tag{20}$$

An approximate equality in the right hand part of Eq. (20) corresponds to the assumption $a \ll R$.
Considering that the angle $\alpha_\perp(\sigma)$ is close to $\frac{\pi}{2}$ we may present $\alpha_\perp$ as a sum of $\frac{\pi}{2}$ and variable part $\tilde\alpha_\perp$:

$$\begin{aligned} \alpha_\perp(\sigma) &= \frac{\pi}{2} + \tilde\alpha_\perp(\sigma), \\ \sin\tilde\alpha_\perp(\sigma) &= -\frac{\sigma\nu(\sigma)}{\sqrt{(\sigma\nu)^2 + (-R+\sigma)^2}}. \end{aligned} \tag{21}$$

Fig. 4 schematically presents the behavior of the helical factor $\nu(\sigma)$ across the toroidal camera.

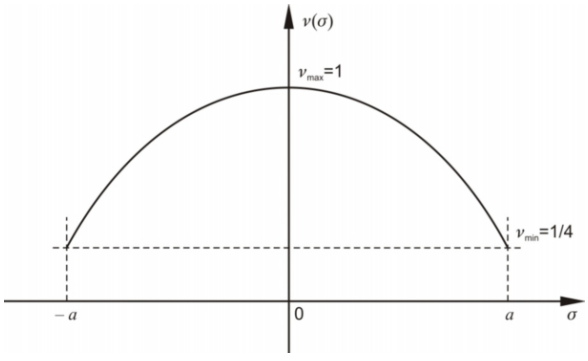

Figure 4. Variations of the helical factor $\nu(\sigma)$ across the toroidal plasma.

Direct estimates show that at $a \sim \frac{R}{2}$ the maximum value of $\tilde\alpha_\perp(\sigma)$ does not exceed 0.1:

$$|\tilde\alpha_\perp(\sigma)|_{\max} \leqslant 0.1. \tag{22}$$

This inequality allows considering $\sin^2\tilde\alpha_\perp$ as a small perturbation in what follows.

4. Polarization angle changes in the sheared plasma: perturbative estimates

The value $\tilde\alpha_\perp(\sigma)$, estimated according to Eq. (22), is small enough to apply the perturbation approach for estimating polarization changes caused by the sheared plasma. Let us substitute the relation $\alpha_\perp(\sigma) = \frac{\pi}{2} + \tilde\alpha_\perp(\sigma)$, Eq. (21), into Eq. (6). Assuming the following, $\cos 2\alpha_\perp(\sigma) = -\cos 2\tilde\alpha_\perp(\sigma)$, $\sin 2\alpha_\perp(\sigma) = -\sin 2\tilde\alpha_\perp(\sigma)$ and neglecting the Faraday term for simplicity, $\Omega_3\left(1+\zeta^2\right)$, one can present Eq. (6) in the form

$$\dot\zeta = -i\Omega_1\zeta + \frac{1}{2}i\Omega_2\left(1-\zeta^2\right) = -i\Omega_1\zeta + f(\zeta), \tag{23}$$

where the value

$$-i\Omega_1\zeta = i\Omega_\perp\zeta\cos 2\tilde\alpha_\perp \tag{24}$$

is a leading term (it tends to $i\Omega_\perp\zeta$, when $\tilde\alpha_\perp \to 0$), whereas the term

$$f(\zeta) = -\frac{1}{2}i\Omega_\perp\left(1-\zeta^2\right)\sin 2\tilde\alpha_\perp, \tag{25}$$

diminishing at $\tilde\alpha_\perp \to 0$, serves as a small perturbation, caused by the sheared plasma:

$$|f(\zeta)| \ll |\Omega_1\zeta|. \tag{26}$$

In these conditions it looks natural to take the value ζ_0, satisfying the equation

$$\dot\zeta_0 = -i\Omega_1\zeta_0 \quad \text{or} \quad \dot\zeta_0 = i\Omega_\perp\zeta_0\cos 2\tilde\alpha_\perp \tag{27}$$

as the zero approximation results in Eq. (23). Eq. (27) results in a similar solution

$$\zeta_0(\sigma) = \zeta(\sigma_0)\exp[i\delta_S(\sigma)], \tag{28}$$

where $\zeta(\sigma_0)$ is an initial value of the complex amplitude ratio $\zeta(\sigma)$ at $\sigma = \sigma_0$ and

$$\delta_S(\sigma) = -\int_{\sigma_0}^{\sigma}\Omega_1(\sigma')d\sigma' = \int_{\sigma_0}^{\sigma}\Omega_\perp(\sigma')\cos 2\tilde\alpha_\perp(\sigma')d\sigma' \tag{29}$$

is the Cotton-Mouton phase difference in the sheared plasma. When $\tilde{\alpha}_\perp = 0$, the phase difference δ_S coincides with the traditional shearless Cotton-Mouton shift

$$\delta_0(\sigma) = \int_{\sigma_0}^{\sigma} \Omega_\perp(\sigma')d\sigma'. \tag{30}$$

It is this value that is presented by equation (1). Taking into account the difference of the wave numbers $k_1 - k_2$ in the case of pure Cotton-Mouton effect and assuming it coincides with $\Omega_\perp$, we have

$$\begin{aligned}\delta_0(\sigma) &= \int_{\sigma_0}^{\sigma} \frac{k_0 X Y^2}{2} d\sigma' = \int_{\sigma_0}^{\sigma} \frac{e^2\omega_p^2 B_0^2}{m^2c^3\omega^3} d\sigma' \\ &= \frac{4\pi e^4}{m^3c^3\omega^3} \int_{\sigma_0}^{\sigma} N_e B_0^2 d\sigma' = \delta_{CM}(\sigma).\end{aligned} \tag{31}$$

The phase shift $\delta_S(\sigma)$, Eq. (29), differs from the shearless phase shift $\delta_0(\sigma)$, Eq. (30), by the value

$$\begin{aligned}\delta_1(\sigma) =& \delta_S(\sigma) - \delta_0(\sigma) = \int_{\sigma_0}^{\sigma} \Omega_\perp(\sigma')[\cos 2\tilde{\alpha}_\perp(\sigma') - 1]d\sigma' \\ =& -2\int_{\sigma_0}^{\sigma} \Omega_\perp(\sigma') \sin^2 \tilde{\alpha}_\perp(\sigma')d\sigma',\end{aligned} \tag{32}$$

which is proportional to $\sin^2 \tilde{\alpha}_\perp$.
Using solution (28) as the zero approximation, we present the solution of Eq. (23) in the form

$$\zeta(\sigma) = \zeta_0(\sigma) + \tilde{\zeta}(\sigma), \tag{33}$$

where $\tilde{\zeta}(\sigma)$ is a small perturbation, disappearing together with $\tilde{\alpha}_\perp$. According to Eqs. (23) and (27), perturbation $\tilde{\zeta}(\sigma)$ obeys the differential equation

$$\dot{\tilde{\zeta}} = -i\Omega_1\tilde{\zeta} + f(\zeta_0 + \tilde{\zeta}). \tag{34}$$

The latter can be transformed into an integral equation

$$\tilde{\zeta}(\sigma) = e^{i\delta_S(\sigma)} \int_{\sigma_0}^{\sigma} f[\zeta_0(\sigma') + \tilde{\zeta}(\sigma')]e^{-i\delta_S(\sigma')}d\sigma'. \tag{35}$$

Applying the method of successive approximations in the form:

$$\begin{aligned}\tilde{\zeta}_{n+1}(\sigma) =& e^{i\delta_S(\sigma)} \int_{\sigma_0}^{\sigma} f[\zeta_0(\sigma') + \tilde{\zeta}_n(\sigma')]e^{-i\delta_S(\sigma')}d\sigma', \\ \tilde{\zeta}_0(\sigma') =& 0,\end{aligned} \tag{36}$$

we have in the lowest approximation ($n = 0$)

$$\begin{aligned}\tilde{\zeta}_1(\sigma) =& e^{i\delta_S(\sigma)} \int_{\sigma_0}^{\sigma} f[\zeta_0(\sigma')]e^{-i\delta_S(\sigma')}d\sigma', \\ \tilde{\zeta}_1(\sigma_0) =& 0.\end{aligned} \tag{37}$$

Substituting $f(\zeta)$ from Eq. (24) and integrating Eq. (37) from the initial value $\sigma_o = -a$ to the output value $\sigma_{\text{out}} = +a$, we obtain

$$\tilde{\zeta}_1(\sigma) = -i \int_{-a}^{+a} \left[\frac{\Omega_\perp}{2} \sin 2\tilde{\alpha}_\perp \left(1 - \zeta_0^2\right)\right] e^{i\delta_S(a) - i\delta_S(\sigma')}d\sigma', \tag{38}$$

where ζ_0 is given by Eq. (28).
Let the initial complex amplitude ratio $\zeta_0(\sigma_0)$ be 1, which corresponds to the linearly polarized initial electrical vector $\mathbf{E}$, directed at the angle $\frac{\pi}{4}$ relative to the axes $\mathbf{e}_1$ and $\mathbf{e}_2$. When $\zeta_0(\sigma_0) = 1$, the first order perturbed solution (37) can be presented as

$$\begin{aligned}\zeta_1(a) =& \zeta_0(\sigma_0)e^{i\delta_S(a)} + \tilde{\zeta}_1(a) = e^{i\delta_S(a)} + \tilde{\zeta}_1(a) \\ =& e^{i\delta_S(a)}\left[1 + e^{-i\delta_S(a)}\tilde{\zeta}_1(a)\right].\end{aligned} \tag{39}$$

The expression $\beta = e^{-i\delta_S(a)}\tilde{\zeta}_1(a)$ happens to be a pure real value:

$$\begin{aligned}\beta =& e^{-i\delta_S(a)}\tilde{\zeta}_1(a) = -i\int_{-a}^{+a} \left[\frac{\Omega_\perp}{2} \sin 2\tilde{\alpha}_\perp \left(1 - \zeta_0^2\right)\right] e^{i\delta_S(\sigma')}d\sigma' \\ =& -i\int_{-a}^{+a} \left[\frac{\Omega_\perp}{2} \sin 2\tilde{\alpha}_\perp \left(e^{i\delta_S(\sigma')} - e^{-i\delta_S(\sigma')}\right)\right] d\sigma' \\ =& \int_{-a}^{+a} \Omega_\perp \sin 2\tilde{\alpha}_\perp(\sigma') \cdot \sin\delta_S(\sigma')d\sigma'.\end{aligned} \tag{40}$$

It means that solution (38) differs from the shearless solution (28) by the phase shift δ_1, Eq. (32), and by the amplitude increment β, Eq. (40).

Numerical modeling of the shear induced phase shift $\delta_1(a)$ was performed on the basis of Eq. (32), using model (21) for the shear angle $\tilde{\alpha}_\perp$. We also used the following quadratic model for the helical factor:

$$\nu(\sigma) = \nu_{\max} - (\nu_{\max} - \nu_{\min}) \left(\frac{\sigma}{a}\right)^2. \tag{41}$$

Specifically, we took $\nu_{\max} = 1$ and $\nu_{\min} = \frac{1}{4}$, so that

$$\nu(\sigma) = 1 - \frac{3}{4}\left(\frac{\sigma}{a}\right)^2. \tag{42}$$

This function is presented in Fig. 4. We also accepted the following parameters

$$\begin{aligned} \delta_0(a) &= 2\Omega_\perp a = \frac{\pi}{4}, \\ \Omega_\perp(\sigma) &= \text{const} = \frac{\pi}{24} \approx \frac{1}{M}, \\ \zeta_0(\sigma_0) &= 1, \\ a &= 3m, \\ R &= 6m. \end{aligned} \tag{43}$$

According to numerical estimates for plasma with parameters (43), reminding those of the ITER project, the value $\delta_1(a)$ happens to be about 0.06 of the Cotton-Mouton phase shift $\delta_0 = 2\Omega_\perp a$, accepted here to be $\frac{\pi}{4}$. Thus, perturbations caused by the sheared plasma, with respect to its numerical value ends up being a smaller percentage of the Cotton-Mouton phase shift. The small value of $\delta_1(a)$ justifies a commonly accepted practice, which is to ignore the influence of the sheared plasma on polarimetric measurements.

In spite of its small size, perturbation $\delta_1(a)$ plays an important role in polarimetric measurements: it determines the potential accuracy of Cotton-Mouton polarimetry.

It is worth pointing out that magnetic lines, presented by the model equations (14) and derived for a simplified plasma of circular cross section, are topologically similar to those in the real tokamak systems, because the magnetic surfaces for real toroidal plasma and the toroidal plasma of circular cross section are in one-to-one correspondence with each other. This property allows concluding that deviations from the shearless Cotton-Mouton effect in both the cases are comparable with respect to their numerical value.

5. Algorithm for improving the accuracy of the polarimetric measurements in conditions of the sheared plasma

The small shear term $\delta_1(a)$ can be reduced by preliminary calculation of the shear angle $\tilde{\alpha}_\perp(\sigma)$ on the basis of modeling of helical magnetic lines, described in Sect. 3 and subtracting the perturbation $\delta_1(a)$ from the measured phase $\delta_{\text{measured}}(a) = \arg\zeta(a)$. The resulting difference $\delta_{\text{measured}}(a) - \delta_1(a)$ can be accepted as the shearless phase difference:

$$\delta_{CM}(a) = \int_{-a}^{a} \Omega_\perp d\sigma = \delta_{\text{measured}}(a) - \delta_1(a). \tag{44}$$

Such a simple method allows decreasing the level of uncertainty in the Cotton-Mouton phase difference by at least 5-10 times. The same is true for the integral $\int_{-a}^{a} N_e \mathbf{B}_\perp^2 d\sigma$, which is estimated on the basis of the Cotton-Mouton phase shift $\delta_{CM}(a)$.

6. Conclusions

The influence of sheared plasma on the Cotton-Mouton effect is analyzed by using the equation for CAR evolution in weakly anisotropic plasma and using a simplified model for helical-like magnetic lines in toroidal plasma, as suggested in [22]. The equation for CPA is solved by perturbative approach, assuming the variable part of the shear angle to be sufficiently small. It is shown that inaccuracy in polarimetric measurements in conditions of the ITER plasma might reach a level that is some percentage of the unperturbed (shearless) solution. A simple algorithm for experimental data processing is suggested, which noticeably allows decreasing the inaccuracy of the polarimetric measurements, caused by the sheared plasma.

Acknowledgements

This work, supported by the European Communities under contract of Association between EURATOM and IPPLM (project P-12), was carried out within the framework of the European Fusion Development Agreement. This work is also supported by the Polish Ministry of Science and High Education (grant Nr 202 249535). The authors express their gratitude to Dr. A. Murari and Dr. D. Mazon for friendly support of our studies which were presented at

a Workshop on plasma polarimetry, held in JET, Culham, UK, 23-24 February 2010. The authors are also indebted to Dr. B. Bieg of the Maritime University in Szczecin, Poland, for encouraging discussions. Lastly, but not least, the authors are cordially thankful to anonymous reviewers for their constructive critical comments.

References

[1] M. Born, E. Wolf, Principles of Optics, 7th edition (Cambridge University Press, Cambridge, 1999)
[2] W.P. Allis, S.J. Buchsbaum, A. Bers, Waves in Anisotropic Plasma (MIT Press, Cambridge, 1963)
[3] V.I. Ginzburg, Propagation of Electromagnetic Waves in Plasma (Gordon & Breach, New York, 1970)
[4] J.M. Donne et al., Rev. Sci. Instrum. 70, 726 (1999)
[5] T.C. Hender et al., Nucl. Fusion 39, 2251 (1999)
[6] T.C. Hender et al., Nucl. Fusion 47, 128 (2007)
[7] S.E. Segre, Plasma Phys. Contr. F. 41, R57 (1999)
[8] S.E. Segre, Phys. Plasmas 2, 2908 (1995)
[9] S.E. Segre, J. Opt. Soc. Am. A 18, 2601 (2001)
[10] S.Huard, Polarization of Light (John Willey & Sons, Masson, 1997)
[11] Yu.A. Kravtsov, B.Bieg, J. Plasma Phys. (in press)
[12] Yu.A. Kravtsov, Soviet Physics - Doklady 13, 1125 (1969)
[13] Yu.A. Kravtsov, O.N. Naida, A.A. Fuki, Phys.-Usp.+ 39, 129 (1996)
[14] A.A. Fuki, Yu.A. Kravtsov, O.N. Naida, Geometrical Optics of Weakly Anisotropic Media (Gordon & Breach, London, New York, 1997)
[15] Yu.A. Kravtsov, Yu.I. Orlov, Geometrical Optics of Inhomogeneous Media (Springer, Berlin, 1990)
[16] Yu.A. Kravtsov, Geometrical Optics in Engineering Physics (Alpha Sci. Int., London, 2005)
[17] Yu.A. Kravtsov, B.Bieg, Plasma Phys. Contr. F. 51, 02200 (2010)
[18] M.M. Popov, Bulletin of the Leningrad University 22, 44 (1969) (in Russian)
[19] V.M. Babich, V.S. Buldyrev, Short-Wavelength Diffraction Theory: Asymptotic Methods (Springer Verlag, Berlin, 1990)
[20] V. Červený, Seismic Ray Theory (Cambridge University Press, Cambridge, 2001)
[21] P. Berczynski, K.Yu. Bliokh, Yu.A. Kravtsov, A. Stateczny, J. Opt. Soc. Am. A 23, 1442 (2006)
[22] Yu.A. Kravtsov, P. Berczynski, Stud. Geophys. Geod. 51, 1 (2007)
[23] Yu.A. Kravtsov, B. Bieg, K.Yu. Bliokh, J. Opt. Soc. Am. A 24, 3388 (2007)
[24] Z.H. Czyz, B. Bieg, Yu.A. Kravtsov, Phys. Lett. A 368, 101 (2007)